



UNIVERSITY OF LEEDS

This is a repository copy of *High Frame-Rate Coherent Diverging Wave Imaging with 2-D Motion Compensation*.

White Rose Research Online URL for this paper:  
<http://eprints.whiterose.ac.uk/143149/>

Version: Accepted Version

---

**Proceedings Paper:**

Nie, L [orcid.org/0000-0002-5796-907X](https://orcid.org/0000-0002-5796-907X), Carpenter, TM, Cowell, DMJ et al. (3 more authors) (2018) High Frame-Rate Coherent Diverging Wave Imaging with 2-D Motion Compensation. In: IUS 2018. IEEE International Ultrasonics Symposium, 22-25 Oct 2018, Kobe, Japan. IEEE . ISBN 978-1-5386-3425-7

<https://doi.org/10.1109/ULTSYM.2018.8579848>

---

© 2018 IEEE. This is an author produced version of a paper published in 2018 IEEE International Ultrasonics Symposium (IUS). Personal use of this material is permitted. Permission from IEEE must be obtained for all other uses, in any current or future media, including reprinting/republishing this material for advertising or promotional purposes, creating new collective works, for resale or redistribution to servers or lists, or reuse of any copyrighted component of this work in other works. Uploaded in accordance with the publisher's self-archiving policy.

**Reuse**

Items deposited in White Rose Research Online are protected by copyright, with all rights reserved unless indicated otherwise. They may be downloaded and/or printed for private study, or other acts as permitted by national copyright laws. The publisher or other rights holders may allow further reproduction and re-use of the full text version. This is indicated by the licence information on the White Rose Research Online record for the item.

**Takedown**

If you consider content in White Rose Research Online to be in breach of UK law, please notify us by emailing [eprints@whiterose.ac.uk](mailto:eprints@whiterose.ac.uk) including the URL of the record and the reason for the withdrawal request.



[eprints@whiterose.ac.uk](mailto:eprints@whiterose.ac.uk)  
<https://eprints.whiterose.ac.uk/>

# High Frame-rate Coherent Diverging Wave Imaging with 2-D Motion Compensation

Luzhen Nie<sup>1</sup>, Thomas M. Carpenter<sup>1</sup>, David M. J. Cowell<sup>1</sup>, James R. McLaughlan<sup>1,2</sup>,  
Arzu A. Çubukçu<sup>3</sup>, and Steven Freear<sup>1</sup>

<sup>1</sup>Ultrasound Group, School of Electronic and Electrical Engineering, University of Leeds, Leeds LS2 9JT, U.K.

<sup>2</sup>Leeds Institute of Cancer and Pathology, University of Leeds, Leeds LS9 7TF, U.K.

<sup>3</sup>East Cheshire NHS Trust, Macclesfield, SK10 3BL, U.K.

E-mail: elln@leeds.ac.uk and s.freear@leeds.ac.uk

**Abstract**—The use of diverging ultrasound waves provides enhanced temporal resolution for cardiac function assessment. However, current image formation techniques using coherent summation, are susceptible to motion artifacts. In this study, we used correlation based 2D motion estimation to perform motion compensation for coherent diverging wave imaging. The accuracy of this motion estimation method was evaluated with Field II simulations, giving root-mean-square velocity errors of  $5.9\% \pm 0.2\%$  and  $19.5\% \pm 0.4\%$  in the axial and lateral directions relative to the maximum velocity of 62.8 cm/s. The results of motion estimation were further processed to render the vector flow map and interpret the motion pattern of the disk. Improvement of the B-mode image quality of a 10 cm *in vitro* tissue mimicking rotating disk was also demonstrated by removing dark imaging artifacts in the compound image.

## I. INTRODUCTION

Ultrasound imaging constitutes an important aid for diagnosis of cardiac dysfunction. It is advantageous over other imaging modalities, such as CT and MRI, being relatively cheap and easily accessible [1]. The list of its applications is expanding to encompass a wider range of diagnostic information including 2-D or 3-D blood flow estimation [2], elasticity of the myocardium [3], wall motion [4] and myocardial perfusion with microbubbles [4].

Instead of using sequential focused beams to form the image line by line, a B-mode image can be reconstructed by transmitting a single diverging wave [5]. The image contrast and resolution can be improved at the receiving side by coherent summation of echoes from multiple transmissions [5]. Diverging wave imaging thus allows for a high frame rate (HRF) up to 10 kHz which is two orders of magnitude faster than the most clinical scanners. This HRF capability underpins a number of novel techniques, such as transient shear wave elastography [6], intracardiac flow velocimetry [7] and coupling myocardium and vortex dynamics [8], for better understanding of cardiac function. However, spatial coherent compounding of diverging waves is susceptible to tissue motion artifacts as highlighted in [9]. Doppler-based methods have been proposed to compensate for motion between multiple diverging wave transmissions prior to compounding, but the maximum velocity without aliasing is bound to  $cPRF/4f_0$  [9], where  $c$  indicates the speed of sound and  $f_0$  is the center frequency of the ultrasound pulse. This

threshold could be small compared to the blood flow in the left ventricle (LV) when correction of microbubble motion is needed in HFR contrast echocardiography using diverging waves [10]. Image registration algorithms such as the one adapted from MRI have been used to correct motion artifacts in coherent diverging wave imaging in [10]. However, the high computational complexity of these algorithms [11] could put restrictions on their real-time implementation. As opposed to registration, correlation-based speckle tracking could be used for motion estimation and compensation in coherent diverging wave imaging but with a lower computational complexity [11].

In this study, a correlation-based method for 2-D motion estimation and compensation was proposed for coherent diverging wave imaging. This enabled a HFR duplex cardiac imaging tool for simultaneous B-mode imaging and 2D vector flow mapping.

## II. MATERIALS AND METHODS

### A. Correlation-based Motion Estimation and Compensation

The motion estimation algorithm used the correlation between diverging wave transmissions prior to compounding. A two-stage speckle tracking method was developed to find the correlation and subpixel displacement between beamformed RF images in the polar grid. The first stage used rigid block matching with correlation correction [12] and this was achieved by multiplying all correlation maps from the pulse sequence for compounding. The second stage used an iterative scheme [13], [14] to improve resolution and accuracy of the motion estimation by recursively decreasing the kernel size and deforming the kernel based on results in the previous iteration. The number of iterations was set to two in this study, with different kernel sizes in each stage as shown in Table II. The resultant motion estimation in each pixel was obtained by linearly interpolating the motion estimation results from the last iteration. Based on these estimated displacements, motion compensation was then performed by aligning image pixels of all low resolution images (LRIs) prior to coherently summing them together. All LRIs with motion were registered to the first LRI within the sequence that is used for coherent compounding.

TABLE I  
PROPERTIES FOR TRANSMISSION

Parameter	Value
Number of elements	64
Pitch size	0.3 mm
Element height	13 mm
Elevation focus	60 mm
Center frequency	2.78 MHz
Bandwidth (−6 dB)	60%
Speed of sound	1540 m/s
Sampling frequency for transmit	160 MHz
Sampling frequency for receive	20 MHz
Excitation signal	4-cycle sinusoid (2.78 MHz)
Tapering function on excitations	Tukey (coefficient: 0.2)
Apodization in transmit	Rectangular window
Apodization in receive	Rectangular window
Angular width $\beta$	90°
Steering angles	(−10°, −8°, −6°, −4°, 4°, 6°, 8°, 10°)
PRF	2 kHz

TABLE II  
PARAMETERS FOR BEAMFORMING AND MOTION ESTIMATION

Parameter	Value
Radial pixel size	38.5 $\mu\text{m}$
Angular pixel size	0.0625°
Window size (1st stage)	152x84
	(radial and angular lines)
Window size (2nd stage)	76x42; 38x21
Window overlap	50%



Fig. 1. Photograph of the rotating disk for *in vitro* experiments.

### B. Imaging Setup

The pulsing scheme for diverging wave imaging was adapted from [9]. A virtual source was placed behind the surface of the probe to emulate a diverging wave. The sector angle which was determinant to the imaging field of view was set to 90° and unchanged during beam steering for compounding. A phased array transducer P4-2v (Verasonics, Inc., WA, USA) was used for Field II simulations [15] and *in vitro* experiments, respectively. It had a −6 dB bandwidth of 60% and a center frequency of 2.78 MHz. The arrangement of steering angles was (−10°, −8°, −6°, −4°, 4°, 6°, 8°, 10°). Pulse repetition frequency (PRF) was set to 2 kHz for both simulations and experimental measurements.

### C. Simulations with a Rotating Disk

A rotating disk with a 10 cm diameter was modelled using Field II. It had a thickness of 10 mm in the elevation direction and was positioned at the depth of 88 mm. In each resolution cell there were 10 scatters, generating fully developed speckle patterns [16]. The disk was rotated anticlockwise with an angular speed of  $4\pi$  rad/s. The maximum velocity of 0.628 m/s corresponding to the maximum blood flow velocity in the LV [17] was achieved at the border of the disk.

The effect of motion compensation was evaluated on compound B-mode images. The accuracy of the motion estimation algorithm was investigated. The root-mean-square (RMS) velocity errors were calculated from ten repeat simulations, with a different noise value added to each repeat (SNR: 30 dB). The RMS velocity errors were then normalized to the maximum speed of the disk. Ultrasound transmission properties are reported in Table I. Beamforming, motion estimation and compensation were performed using parameters in Table II.

### D. In vitro Experiments with a Rotating Disk

The University of Leeds Ultrasound Array Research Platform II (UARP II) was used for experimental measurements. It is capable of arbitrary waveform generation on each channel [18], [19].

A tissue mimicking disk as shown in Fig. 1 was cast [22] with a speed of sound 1540 m/s and attenuation value of 0.55 dB/MHz/cm. It had the same diameter of 10 cm as used for simulations and also had four equidistant 12.8-mm anechoic cysts (filled with water) located at 32 mm relative to the disk center. The disk was driven by a stepper motor with the same angular speed of  $4\pi$  rad/s. Peak negative pressures were measured with a 0.2 mm needle hydrophone (Precision Acoustics, Dorchester, UK) in water to determine the mechanical index [23] of 0.12 (*in situ*). Parameters for beamforming, motion estimation and compensation were identical to those used for simulations as reported in Table II.

## III. RESULTS

### A. Simulations

Fig. 2 shows the compound images of the rotating disk before and after the use of motion compensation when using 8 diverging waves. Imaging artifacts are noticeable as shown in Fig. 2 (a), with two dark regions and smearing background shown in the imaging field. With the application of motion compensation, the disk becomes interpretable with uniform speckle distribution and improved border delineation.

The accuracy of the motion estimation was investigated by calculating the RMS velocity errors with ten repeat simulations. The RMS velocity errors were  $5.9\% \pm 0.2\%$  and  $19.5\% \pm 0.4\%$  for the axial and lateral directions, respectively. In addition to improving the quality of the compound image, the

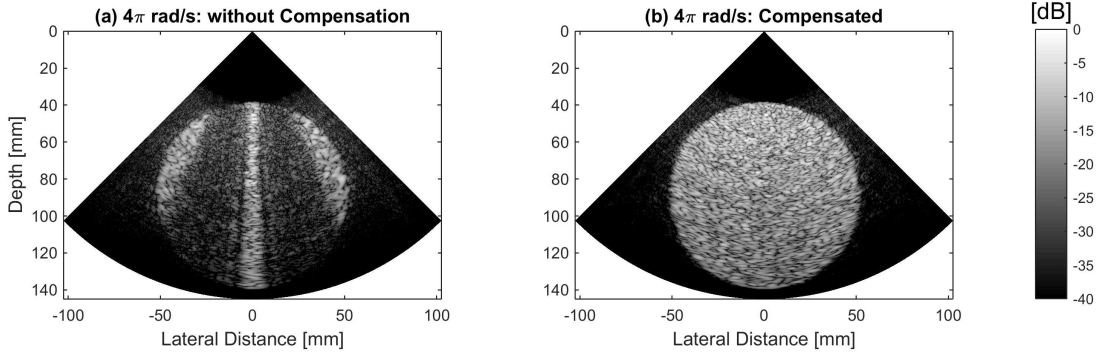


Fig. 2. Field II simulations: compound images of the rotating disk before and after motion compensation.

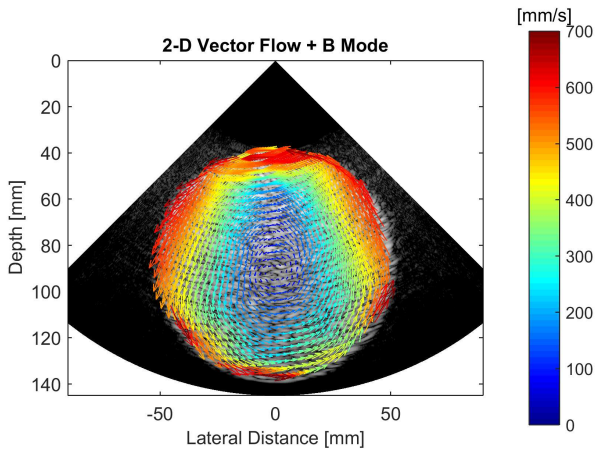


Fig. 3. Field II simulations: vector flow map superimposed onto the compound B-mode image.

results of motion estimation for compensation were encoded to depict the motion pattern of the disk as shown in Fig. 3. The capability of simultaneous B-mode imaging and 2D vector flow mapping could benefit HFR contrast-enhanced echocardiography using diverging waves [1].

### B. *In vitro* Experiments

Fig. 4 shows the compound images of the *in vitro* disk in the static state, in the rotating state without and with motion compensation, respectively. Without the application of motion compensation, the similar imaging artifacts as shown in Fig. 2 (a) can be found in Fig. 4 (b). The proposed method restored the disk in the presence of motion as shown in Fig. 4 (c).

## IV. DISCUSSION

Doppler, registration and correlation based methods could be used for motion compensation in coherent diverging wave imaging. Doppler based methods, however, would be limited by aliasing when correction of microbubble motion is needed in the LV for HFR contrast-enhanced echocardiography [10].

Implementation of coherent diverging wave imaging with motion correction on commercial scanners will not be straightforward, as they not only require the change of pulsing schemes, but they also bring challenges in data transfer and storage. With the continued maturity of open ultrasound platforms [24], the proposed method in this study could be implemented in real time when using a simple cross-correlator [25]. Comparisons between the method in the current study and image registration based methods warrant more investigations in terms of image resolution, contrast ratio and computational complexity.

*In vivo* studies will be entailed for evaluating the practical value of the method in this study for HFR contrast-enhanced echocardiography in the future. Coupling myocardium and vortex dynamics has been suggested for early diagnosis of LV filling impairment [8], but this requires a high temporal resolution. With the same pulse sequence, HFR B-mode imaging and 2-D vector flow mapping have been obtained simultaneously at 250 Hz as demonstrated in Section III. When using microbubbles, the proposed method could facilitate a HFR cardiac imaging tool using diverging waves, which could drastically improve our understanding of cardiac function by coupling myocardial motion, vortex dynamics in the LV and even microbubble-assisted myocardial perfusion.

## V. CONCLUSIONS

The present study described the implementation of a correlation-based method for coherent diverging wave imaging in the presence of motion artifacts. Motion estimation was performed between diverging waves prior to compounding and the estimated displacement was used to counter-shift the motion to achieve coherent summation. The improved image quality has been obtained in both simulations and *in vitro* experiments for a disk rotated at  $4\pi$  rad/s.

## VI. ACKNOWLEDGEMENT

This work was supported by the EPSRC under Grant EP/P023266/1 and EP/N034813/1. J. R. McLaughlan would like to acknowledge support from an EPSRC Innovation Fellowship EP/S001069/1.

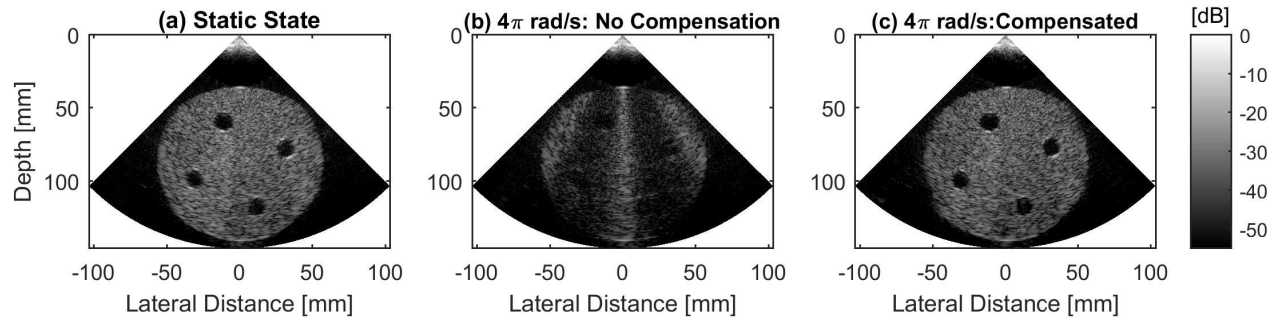


Fig. 4. Compound images of the *in vitro* disk in the (a) static state, the rotating state (b) without and (c) with motion compensation.

## REFERENCES

- [1] M. E. Toulemonde, R. Corbett, V. Papadopoulou, N. Chahal, Y. Li, C. H. Leow, D. O. Cosgrove, R. J. Eckersley, N. Duncan, R. Senior *et al.*, "High frame-rate contrast echocardiography: In-human demonstration," *JACC: Cardiovascular Imaging*, vol. 11, no. 6, pp. 923–924, 2018.
- [2] B. F. Osmanski, D. Maresca, E. Messas, M. Tanter, and M. Pernot, "Transthoracic ultrafast doppler imaging of human left ventricular hemodynamic function," *IEEE Transactions on Ultrasonics, Ferroelectrics, and Frequency Control*, vol. 61, no. 8, pp. 1268–1275, August 2014.
- [3] J. Grondin, V. Sayseng, and E. E. Konofagou, "Cardiac strain imaging with coherent compounding of diverging waves," *IEEE Transactions on Ultrasonics, Ferroelectrics, and Frequency Control*, vol. 64, no. 8, pp. 1212–1222, Aug 2017.
- [4] R. Senior, H. Becher, M. Monaghan, L. Agati, J. Zamorano, J. L. Vanoverschelde, and P. Nihoyannopoulos, "Contrast echocardiography: evidence-based recommendations by european association of echocardiography," *European Journal of Echocardiography*, vol. 10, no. 2, pp. 194–212, 2009.
- [5] C. Papadacci, M. Pernot, M. Couade, M. Fink, and M. Tanter, "High-contrast ultrafast imaging of the heart," *IEEE Transactions on Ultrasonics, Ferroelectrics, and Frequency Control*, vol. 61, no. 2, pp. 288–301, February 2014.
- [6] O. Villemain, M. Correia, E. Mousseaux, J. Baranger, S. Zarka, I. Podetti, G. Soulat, T. Damy, A. Hagège, M. Tanter, M. Pernot, and E. Messas, "Myocardial stiffness evaluation using noninvasive shear wave imaging in healthy and hypertrophic cardiomyopathic adults," *JACC: Cardiovascular Imaging*, 2018. [Online]. Available: <http://imaging.onlinejacc.org/content/early/2018/03/09/j.jcmg.2018.02.002>
- [7] J. Voorneveld, A. Muralidharan, T. Hope, H. J. Vos, P. Kruizinga, A. F. W. van der Steen, F. J. H. Gijsen, S. Kenjeres, N. de Jong, and J. G. Bosch, "High frame rate ultrasound particle image velocimetry for estimating high velocity flow patterns in the left ventricle," *IEEE Transactions on Ultrasonics, Ferroelectrics, and Frequency Control*, pp. 1–1, 2017.
- [8] J. Faurie, M. Baudet, J. Pore, G. Cloutier, F. Tournoux, and D. Garcia, "Coupling myocardium and vortex dynamics in diverging-wave echocardiography," *IEEE Transactions on Ultrasonics, Ferroelectrics, and Frequency Control*, pp. 1–1, 2018.
- [9] J. Pore, D. Posada, A. Hodzic, F. Tournoux, G. Cloutier, and D. Garcia, "High-frame-rate echocardiography using coherent compounding with doppler-based motion-compensation," *IEEE Transactions on Medical Imaging*, vol. 35, no. 7, pp. 1647–1657, July 2016.
- [10] M. Toulemonde, W. C. Duncan, A. Stanziola, V. Sboros, Y. Li, R. J. Eckersley, S. Lin, M. X. Tang, and M. Butler, "Effects of motion on high frame rate contrast enhanced echocardiography and its correction," in *2017 IEEE International Ultrasonics Symposium (IUS)*, Sept 2017, pp. 1–4.
- [11] B. Heyde, R. Jasaityte, D. Barbosa, V. Robesyn, S. Bouchez, P. Wouters, F. Maes, P. Claus, and J. D'hooge, "Elastic image registration versus speckle tracking for 2-d myocardial motion estimation: A direct comparison in vivo," *IEEE Transactions on Medical Imaging*, vol. 32, no. 2, pp. 449–459, Feb 2013.
- [12] L. Nie, S. Harput, D. M. J. Cowell, and S. Freear, "Velocity estimation error reduction in stenosis areas using a correlation correction method," in *2016 IEEE International Ultrasonics Symposium (IUS)*, Sept 2016, pp. 1–4.
- [13] L. Niu, M. Qian, K. Wan, W. Yu, Q. Jin, T. Ling, S. Gao, and H. Zheng, "Ultrasonic particle image velocimetry for improved flow gradient imaging: algorithms, methodology and validation," *Physics in Medicine & Biology*, vol. 55, no. 7, p. 2103, 2010.
- [14] J. Westerweel and F. Scarano, "Universal outlier detection for piv data," *Experiments in Fluids*, vol. 39, no. 6, pp. 1096–1100, 2005.
- [15] J. A. Jensen and N. B. Svendsen, "Calculation of pressure fields from arbitrarily shaped, apodized, and excited ultrasound transducers," *IEEE Transactions on Ultrasonics, Ferroelectrics, and Frequency Control*, vol. 39, no. 2, pp. 262–267, March 1992.
- [16] K. L. Gammelmark and J. A. Jensen, "2-d tissue motion compensation of synthetic transmit aperture images," *IEEE Transactions on Ultrasonics, Ferroelectrics, and Frequency Control*, vol. 61, no. 4, pp. 594–610, April 2014.
- [17] E. Beeri, S. E. Maier, M. J. Landzberg, T. Chung, and T. Geva, "In vivo evaluation of fontan pathway flow dynamics by multidimensional phase-velocity magnetic resonance imaging," *Circulation*, vol. 98, no. 25, pp. 2873–2882, 1998.
- [18] D. Cowell and S. Freear, "Quinary excitation method for pulse compression ultrasound measurements," *Ultrasonics*, vol. 48, no. 2, pp. 98–108, 2008.
- [19] P. R. Smith, D. M. J. Cowell, and S. Freear, "Width-modulated square-wave pulses for ultrasound applications," *IEEE Transactions on Ultrasonics, Ferroelectrics, and Frequency Control*, vol. 60, no. 11, pp. 2244–2256, November 2013.
- [20] C. Adams, S. Harput, D. Cowell, T. M. Carpenter, D. M. Charutz, and S. Freear, "An adaptive array excitation scheme for the unidirectional enhancement of guided waves," *IEEE Transactions on Ultrasonics, Ferroelectrics, and Frequency Control*, vol. 64, no. 2, pp. 441–451, Feb 2017.
- [21] S. Harput, M. Arif, J. McLaughlan, D. M. J. Cowell, and S. Freear, "The effect of amplitude modulation on subharmonic imaging with chirp excitation," *IEEE Transactions on Ultrasonics, Ferroelectrics, and Frequency Control*, vol. 60, no. 12, pp. 2532–2544, Dec 2013.
- [22] L. Nie, S. Harput, D. M. J. Cowell, T. M. Carpenter, J. R. McLaughlan, and S. Freear, "Combining acoustic trapping with plane wave imaging for localized microbubble accumulation in large vessels," *IEEE Transactions on Ultrasonics, Ferroelectrics, and Frequency Control*, vol. 65, no. 7, pp. 1193–1204, July 2018.
- [23] C. C. Church, "Frequency, pulse length, and the mechanical index," *Acoustics Research Letters Online*, vol. 6, no. 3, pp. 162–168, 2005.
- [24] E. Boni, A. C. H. Yu, S. Freear, J. A. Jensen, and P. Tortoli, "Ultrasound open platforms for next-generation imaging technique development," *IEEE Transactions on Ultrasonics, Ferroelectrics, and Frequency Control*, pp. 1–1, 2018.
- [25] J. Luo and E. E. Konofagou, "A fast normalized cross-correlation calculation method for motion estimation," *IEEE Transactions on Ultrasonics, Ferroelectrics, and Frequency Control*, vol. 57, no. 6, pp. 1347–1357, June 2010.